Hindawi Publishing Corporation
Advances in Optical Technologies
Volume 2014, Article ID 167129, 8 pages
http://dx.doi.org/10.1155/2014/167129

Research Article

Implementation of a Phase Only Spatial Light Modulator as an Atmospheric Turbulence Simulator at 1550 nm

Carlos Font,[1] Freddie Santiago,[2] G. Charmaine Gilbreath,[1] David Bonanno,[1] Blerta Bajramaj,[1] Christopher Wilcox,[3] Sergio Restaino,[3] and Scott Mathews[4]

[1] *U. S. Naval Research Laboratory, Freespace Photonics Communications Office, Code 5505, Washington, DC 20375, USA*
[2] *Sandia National Laboratories, 1515 Eubank Boulevard, SE Albuquerque, NM 87123, USA*
[3] *U. S. Naval Research Laboratory, Wavefront Sensing & Control, Code 7216, Albuquerque, NM 87101, USA*
[4] *Electrical Engineering and Computer Sciences Department, The Catholic University of America, Washington, DC 20064, USA*

Correspondence should be addressed to Carlos Font; carlos.font@nrl.navy.mil

Received 25 February 2014; Revised 12 June 2014; Accepted 30 June 2014; Published 6 August 2014

Academic Editor: Partha P. Banerjee

Modeling and simulating atmospheric turbulence in a controlled environment have been a focus of interest for scientists for decades. The development of new technologies allows scientists to perform this task in a more realistic and controlled environment and provides powerful tools for the study and better understanding of the propagation of light through a nonstatic medium such as the atmosphere. Free space laser communications (FSLC) and studies in light propagation through the atmosphere are areas which constantly benefit from breakthroughs in technology and in the development of realistic atmospheric turbulence simulators, in particular (Santiago et al. 2011). In this paper, we present the results from the implementation of a phase only spatial light modulator (SLM) as an atmospheric turbulence simulator for light propagation in the short-wave infrared (SWIR) regime. Specifically, we demonstrate its efficacy for its use in an FSLC system, at a wavelength of 1550 nm.

1. Introduction

The atmosphere is a nonhomogeneous medium that has properties sensitive to changes in pressure, temperature, humidity, and wind speed and direction. Its layered nature and sensitivity to different variables generate turbulent fluctuations in the refractive index of the atmosphere. These turbulent fluctuations are considered to be the principal contributors of the phase fluctuations in traveling optical waves [1–4]. For decades, scientists have been studying and modeling atmospheric turbulence to obtain a better understanding of its properties and behavior. Atmospheric turbulence simulators (ATS) are powerful tools enabling researchers to evaluate and predict the performance of optical systems prior to field implementation. Some of the most common methods used to simulate atmospheric turbulence are rotating phase plates etched with phase screens, hot plates, or liquid crystal modulators. The use of hot plates is limited by the inability to accurately estimate or precisely control the degree of atmospheric turbulence introduced to the optical path. Rotating phase plates are extremely costly and limited by the number of phase screens. Recent improvements to Liquid Crystal-based Spatial Light Modulators (LCSLM) have made these types of modulators more useful as an ATS for system calibration and design [5–7]. This is because a given set of aberrations can be carefully introduced and controlled in a laboratory environment for both frozen phase screen studies and real-time turbulence emulations [8]. This paper describes the implementation of such an LCSLM in the short-wave infrared (SWIR) in a laboratory test-bed.

The ATS was designed to enable the evaluation of the effect of atmospheric turbulence on wave propagation in the SWIR regime for FSLC systems and on free-space near-infrared communication links. This simulator innovation is based on a recently patented method for generating atmospheric turbulence [9]. This method produces a time varying phase screen which represents atmospheric turbulence and it is generated by using Karhunen-Loeve polynomials and

a splining technique for generating temporal functions of the noise factor for each Zernike polynomial [10]. These generated phase screens are projected on the liquid crystal spatial light modulator. The atmospheric turbulence simulator with the implemented software enables the user to control different parameters such as the aperture of the optical system, the Fried parameter, r_0, and the coherence time of the atmosphere, τ_0 [5, 6]. The atmospheric turbulence can be adjusted from weak to strong turbulence conditions by adjusting and controlling the r_0 and/or the optical system aperture. The NRL software algorithm also generates controlled phase aberrations based on Zernike polynomials [1] for system alignment and fine-tuning.

2. Spatial Light Modulator

For this work, we used a PLUTO-Telco spatial light modulator (SLM) from HOLOEYE, Inc. The SLM is a reflective Liquid Crystal on Silicon (LCOS) microdisplay with 1920 × 1080 pixels resolution and has a pixel pitch of 8 μm. The device is optimized to provide a phase shift above 2π for wavelengths up to 1550 nm with approximately a 60% reflectivity. This device is addressed as an external monitor at a refresh rate of 60 Hz using a HDTV graphics card. HDTV resolution images are sent to the device via a digital video interface (DVI). The unit is shown in Figure 1.

The PLUTO-TELCO SLM is a high-resolution phase display that allows independent control of each pixel and modulates the incident polarized light by birefringence. A birefringent material has different indices of refraction depending on the polarization and the direction of the propagation of the light. The molecules in the LCOS have anisotropic characteristics, which enables the birefringence for incident polarized light. This specific model offers 256 gray levels (8-bits) enabling the generation of phase screens with a reliable modulation depth of 2π. Phase screens for this work were generated by the ATS software developed at NRL as previously referenced. These generated phase screens are displayed on a secondary computer monitor that matches the number of pixels of the SLM (Figure 2(a)). The information is sent to each pixel generating a visible pattern on its surface as seen in Figure 2(b).

The PLUTO-TELCO SLM contains three main components which need to be configured to achieve optimal performance. These are (1) the potentiometer, (2) the upload "sequences," and (3) the gamma tables.

The depth of modulation of a given pixel is controlled by the applied voltage. The potentiometer enables us to set the operational voltage range for a given application. By limiting the voltage range, we can reduce flickering as well as modulate phase depth. The degree of total bit-depth achievable by the device can be changed by using different "sequences" sizes. A long "sequence" offers a higher number of different states for each and a shorter "sequence" will offer lower number of states. For example, an "18-6 sequence" can be used to provide 1216 different values for a given look-up table (LUT). A "5-5 sequence" will provide 192 LUT values. The shorter "sequence" offers stability because it decreases the flicker noise in comparison with the long "sequence." The longer "sequence" allows a higher number of states which offers a greater resolution in phase modulation. In this work, the "5-5' sequence" was selected.

Finally, an optimized gamma correction table is necessary to ensure the linearity of the phase response of the SLM. Like the potentiometer, the gamma correction table also helps to pin the response of the device to an exact phase value. Figure 3(a) shows the measured phase response at 1550 nm using a linear gamma table (top left) compared to the corrected gamma table based on data measured in the laboratory (top right). The corresponding phase responses are shown below the graphs. It should be noted that these images are a collection of cross sections of a set of images collected while sending the LUT values to the device at a preselected set of steps, 256 steps for our case. These measurements images (bottom left) clearly show a nonlinear response from the SLM. The corrections to generate a calibrated gamma table are created by taking measurements in the laboratory and applying the software (PhaseCam) provided by the manufacturer of the liquid crystal for the calculations of the LUT table. The resulting LUT values as a function of gray levels for the corrected table are shown in (Figure 3 (top left)). The image at the bottom right of Figure 3 shows a linear phase response from 0 to 2π, which is required to achieve optimal diffraction efficiency by the device.

To complete the calibration process before data for the experiment was taken, a diffraction test was performed using the SLM. For this test a diffraction grating was generated on the surface of the SLM, as shown in Figure 2. The performed test diffracted 72% of the incident light into the 1st order, as seen in Figure 4. This measurement is consistent with the vendor's claims. At this point, the SLM was inserted into the experimental setup as shown in Figure 5.

3. Laboratory Experiment and Testing Procedure

An optical bench was configured in the laboratory to investigate the impact of controlled levels of turbulence and wavefront aberrations on a 1550 nm beam. To do this, we used a 1555 nm coherent light source, coated optical elements for the corresponding wavelengths, the SLM to control aberrations, a Shack-Hartman detector, and cameras. The optical configuration is shown in Figure 5. Starting with the light source, we selected a 1555 nm distributed feedback laser (DFB) with a polarization maintaining (PM) fiber. PM fiber components and selected optics were used and were necessary to maintain matching linear polarization through the system and to present a 0° horizontal polarization angle to the LCSLM. These components with careful alignment were required to achieve optimal performance. A commercial collimator with a beam diameter of 6.9 mm and a full-angle divergence of 0.016° was used to launch the light into free space. This diameter was selected to match the 7 mm diameter phase screens generated on the SLM display.

This particular LC SLM is a reflective device. Therefore, we built a Michelson Interferometer using the LC SLM as

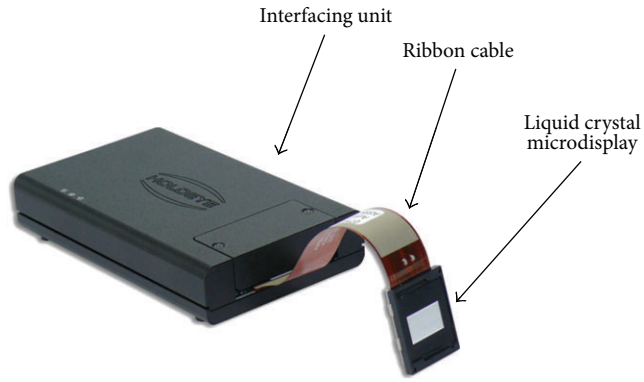

Figure 1: The SLM used for this work is shown above. The unit is the high resolution phase only spatial light modulator from HoloEye, Inc.

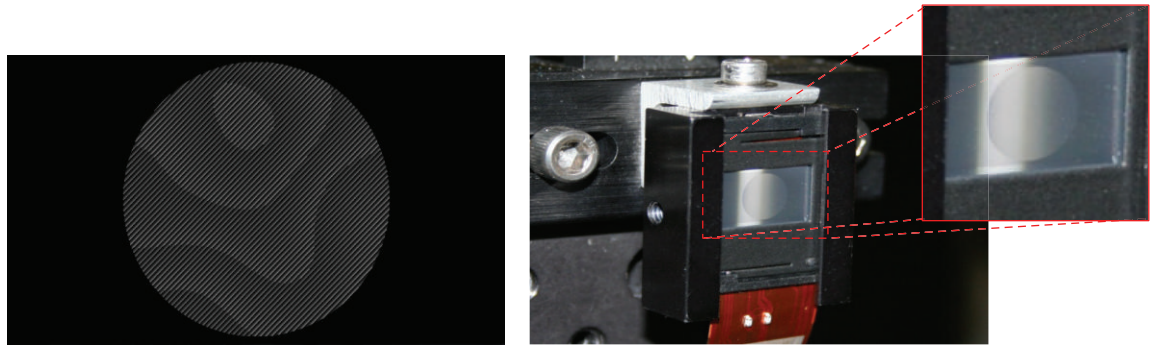

(a) (b)

Figure 2: (a) A screenshot is shown of the computer monitor of the generated phase screen. (b) The image of the LC SLM shows the pattern formed on its surface after the information which generated the phase screen seen on the right was sent to the device.

the variable arm of the interferometer and a gold coated, flat mirror in the reference arm. A Michelson Interferometer reflects light at 0° incidence angle, thereby enabling the use of the entire dynamic range of the device. The beam was then directed through a series of beamsplitters to send portions of the light to four different detection configurations. As shown in Figure 5, the transmissive part of the beam after the first beamsplitter, B1, was sent to the SLM and the reflected portion of the beam was sent to the reference mirror, M2. The light from the reflected beam was directed to (1) a CamIR1550 infrared camera with an aperture-matched telescope, which recorded the interferogram to assess wavefront characteristics at 1550 nm; (2) a Shack Hartman Wavefront Sensor (SHWFS) for wavefront reconstruction; and (3) a Spiricon Infrared Camera to record the Point Spread Function (PSF) of the laser beam also at 1550 nm, without interference from the reference beam. The reference beam was blocked at the time to measure the PSF of the laser beam to avoid interference effects on the measurements.

The two scientific cameras used in the experimental configuration were a CCD sensor from Applied Scintillation Technologies (CamIR1550) and a Silicon CCD from Spiricon Inc. The CamIR1550 is an inexpensive CCD which has 752 (H) × 582 (V) pixels with an effective pixel size of 20 μm. The USB Spiricon L230 is a Silicon CCD which has 1616 (H) × 1216 (V) pixels. We also used a Shack-Hartman Wave front Sensor (SHWFS) consisting of a microlens array of 127 subapertures in a hexagonal geometry, a focal length of 18 mm and a 300 μm pitch. FrontSurfer from OKO Technologies was the software implemented for wavefront reconstruction and analysis.

The LC SLM was controlled using the Atmospheric Turbulence Simulator (ATS) application developed by Wilcox at the Naval Research Laboratory [5, 6]. Modifications to the ATS software were needed to enable integration of the SLM into our system for our application. The NRL ATS software can be customized to control the SLM to produce the phase modulations and simulated turbulence levels through a Graphical User Interface (GUI). The application provides menu-driven options to select the order of aberrations to be generated based on the Zernike polynomials and can be used for fine-tuning the system's optical alignment. The ATS software also provides the option to choose the degree of atmospheric turbulence to be simulated (weak or strong turbulence). This value can be generated by changing parameters like the Fried parameter (r_0) and the system's aperture (D). Different algorithms to generate turbulence can also be used. The algorithms available in the ATS are Zernike Modes,

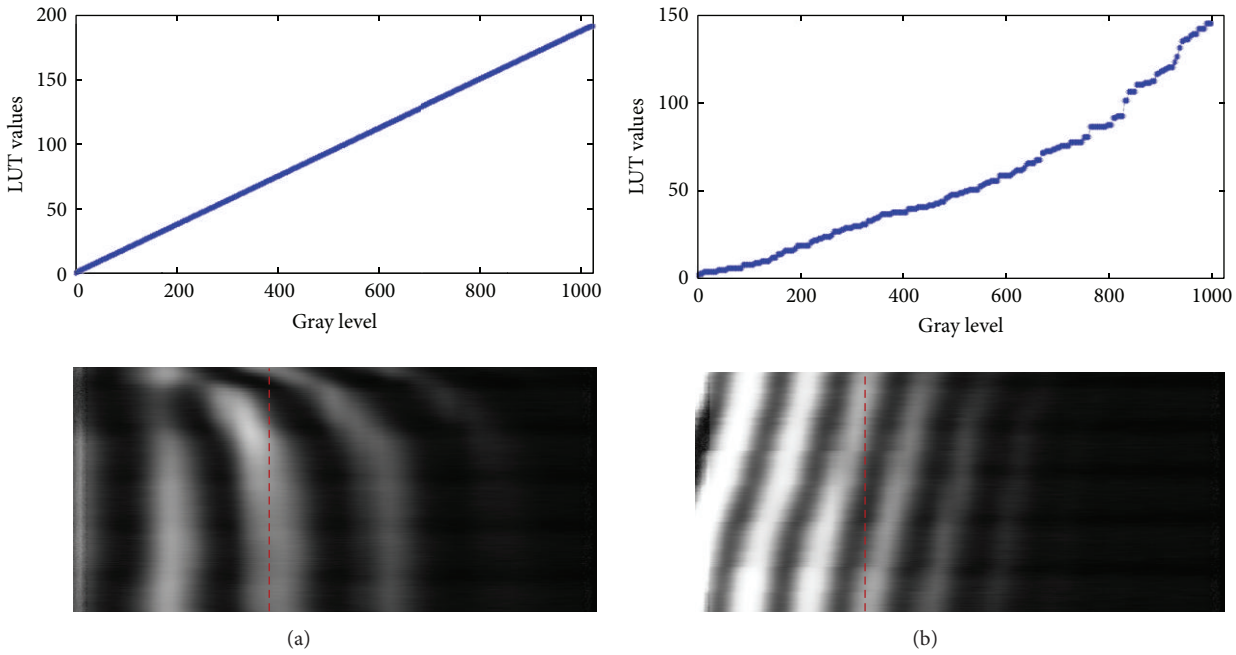

Figure 3: Left: a linear gamma table applied to the FLCSLM with its recorded phase response is shown. Right: the corrected gamma table is shown based on 256 measurement sets calibrated by the manufacturer's algorithm. The corresponding linear phase response from 0 to 2π is shown in the image below the graph. The data presented in this figure was generated for calibration purposes using an algorithm provided by the company, which generated a 10-bit vector. The LUT values table used in the ATS was an 8-bit vector to make it compatible with the NRL software.

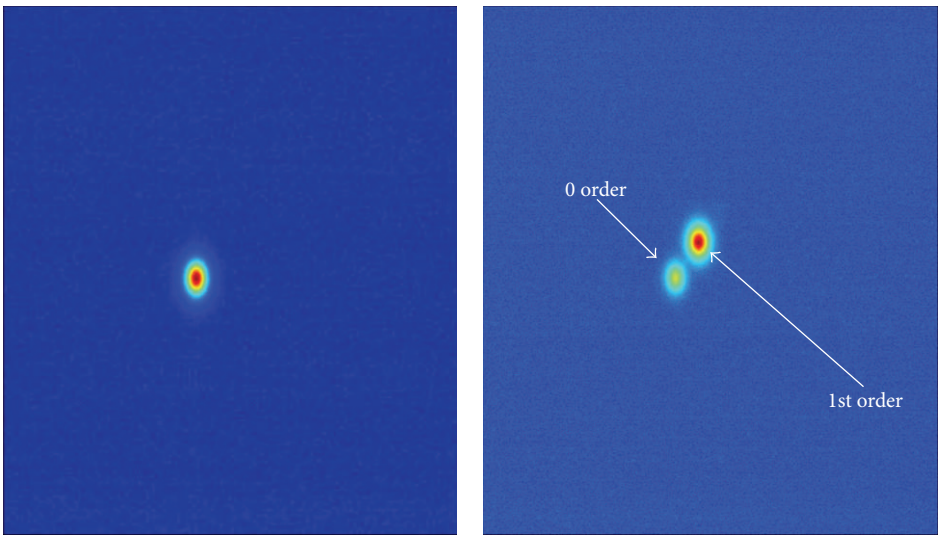

Figure 4: (a) Light is reflected from the SLM into the Spiricon camera with no diffraction grating phase screen displayed on the SLM. (b) Light is reflected from the SLM displaying a diffraction grating phase screen. The gamma table for a linear phase response has been uploaded to the SLM. This shows 72% diffraction efficiency into the first order.

Karhunen-Loeve Modes, and Frozen Seeing [6]. The GUI of Atmospheric Turbulence Simulator (ATS) software is shown in Figure 6, which illustrates the menu options.

After the optical alignment was completed the SHWFS was used to test the quality of the reference beam and the wavefront of the reflected beam from the SLM. The ATS software was then used to generate phase screens with specific aberrations based on the Zernike polynomials. In order to achieve a greater separation between the diffracted orders for easier identification and analysis, it was necessary to add a tip and tilt bias into each phase screen. These phase screens were then transmitted into the SLM. Figure 7 shows

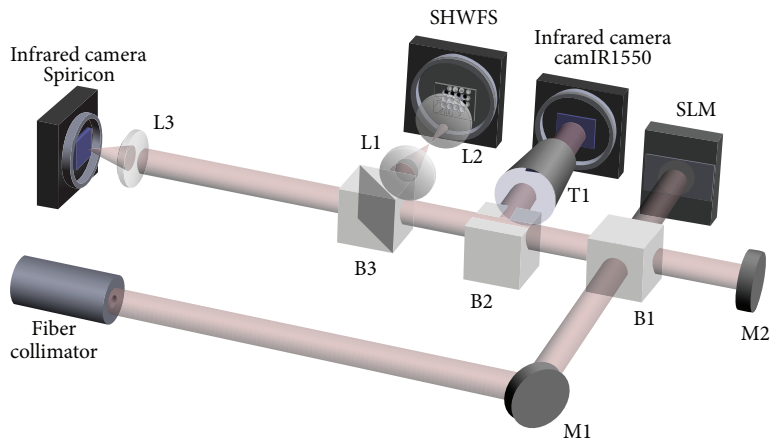

Figure 5: Optical bench configuration for calibration of the phase only SLM system is shown. Three diagnostics are provided by this setup: infrared camera CamIR1550 to record the interference patterns at 1550 nm; a Shack-Hartmann Wavefront Sensor for wavefront reconstruction; and a Spiricon Infrared Camera to detect and record Point Spread Functions at 1550 nm.

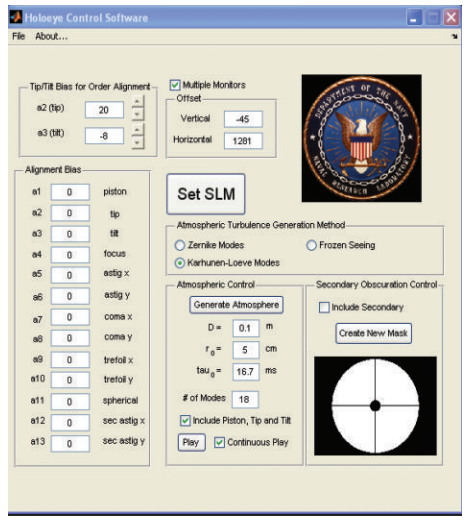

Figure 6: A frame is shown from the Graphical User Interface (GUI) from the Atmospheric Turbulence Simulator (ATS). This GUI enables interactive control of phase screens generated and displayed on the SLM.

some examples of the performed test including the generated phase screen, the PSF, and the generated interferogram for each generated phase screen. Different aberrations including coma, focus, and astigmatism, and others were tested and verified.

4. Results

The ATS software was used to generated a set of random phase screens which simulate atmospheric turbulence by using the Fried parameter (r_0) and the aperture system (D). The multimedia file, Video 1 (see Supplementary Materials available online at http://dx.doi.org/10.1155/2014/167129), Figure 8(a), shows the dynamic random phase screens that were generated by the ATS software. The effects of those phase screens on the light beam are shown in Figure 8(b) where they obsere the PSF variationes in shape, location, and quality. A diagnostic in the form of using the corresponding interferograms is shown in Figure 8(c). In this video clip, the characteristic fringe patterns for different combinations of the Zernikes resulting from turbulence-like randomized phase changes is evident and enables the researcher to systematically diagnose the impact of specfic combinations on beam behavior.

To deterministically explore experimentally the relationship between r_0 and the aperture of the system, we varied D/r_0 for different combinations of aberration types. The ratios evaluated were 1 : 1, 2 : 1, and 10 : 1, where D was fixed at 10 cm as per the experimental bench, and r_0 was varied.

Some results are shown in Figure 9. Figure 9(a) shows that in the corresponding data with a ratio D/r_0 of 1 there is a little disturbance introduced into the laser beam, mostly in the low order Zernikes polynomials. For the second data set, also in Figure 9(b), a ratio of 2 was used by changing the Fried

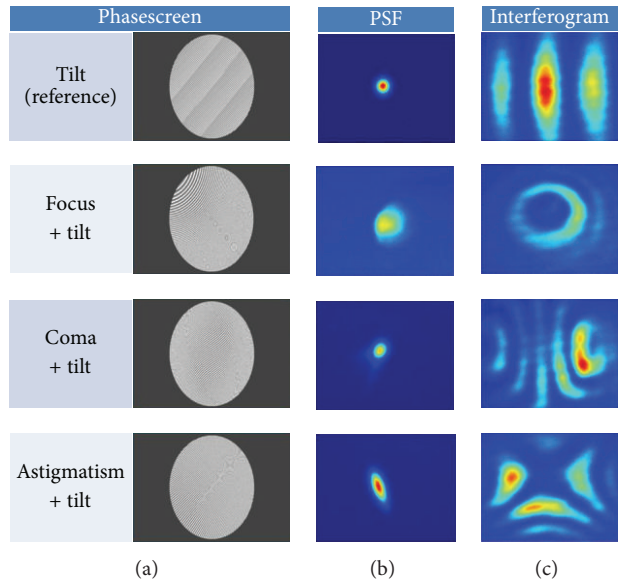

Figure 7: This figure compares results from the diagnostic sensors at 1550 nm: (a) generated phase screens; (b) respective point spread functions; (c) corresponding interferograms.

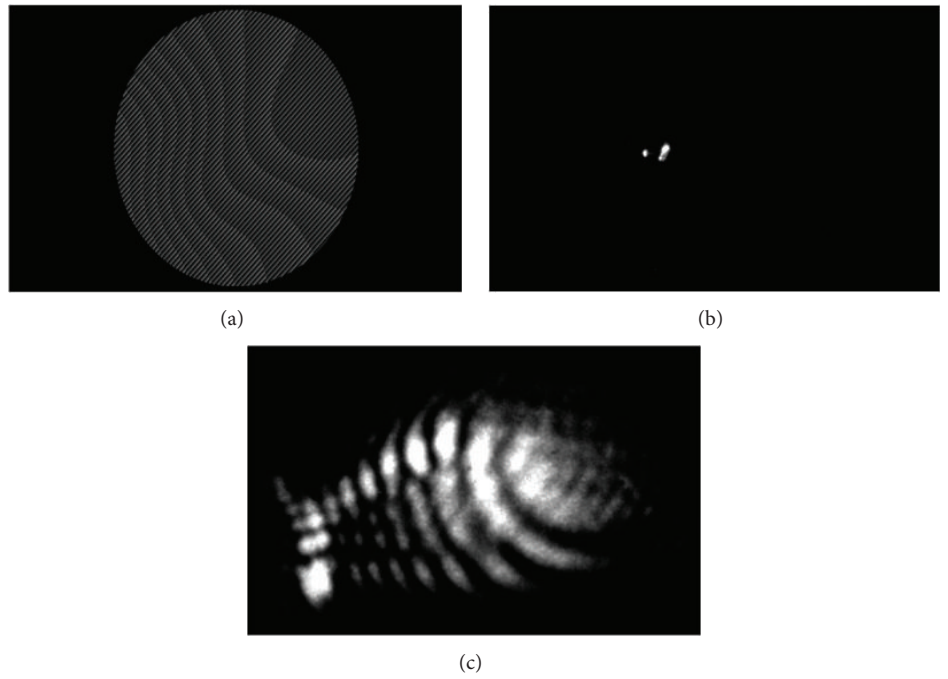

Figure 8: This multimedia file (Supplementary Video 1) is showing the impact of randomized phase screens on the 1550 nm laser beam. They are: (a) Generated random phase screen; (b) The point spread function (PSF) of the beam after been diffracted; and (c) The generated interferogram using the generated random phase screen. (Supplementary Video 1, QuickTime, 8.3 MB). Click on the image to activate the video.

parameter to 5 cm. Again, we can discern that the disturbance is detected in the low order Zernikes polynomials, but with more pronounced effects in the magnitudes. At this ratio, the system's ON-OFF transitions are also more evident (note the scales of the y-axis). The greatest impact on the beam was predicatably evident by the ratio of 10 : 1, Figure 9(c), where the Fried parameter was set to 1 cm. This setting would be equivalent to strong turbulence effects, while Figure 10 show the variance on the magnitude of the Zernike polinomials for each case mention above. From Figure 9 we can see that the turbulence is not only there, but it shows a clear effect in the measurements, as indicated by Figure 10. These

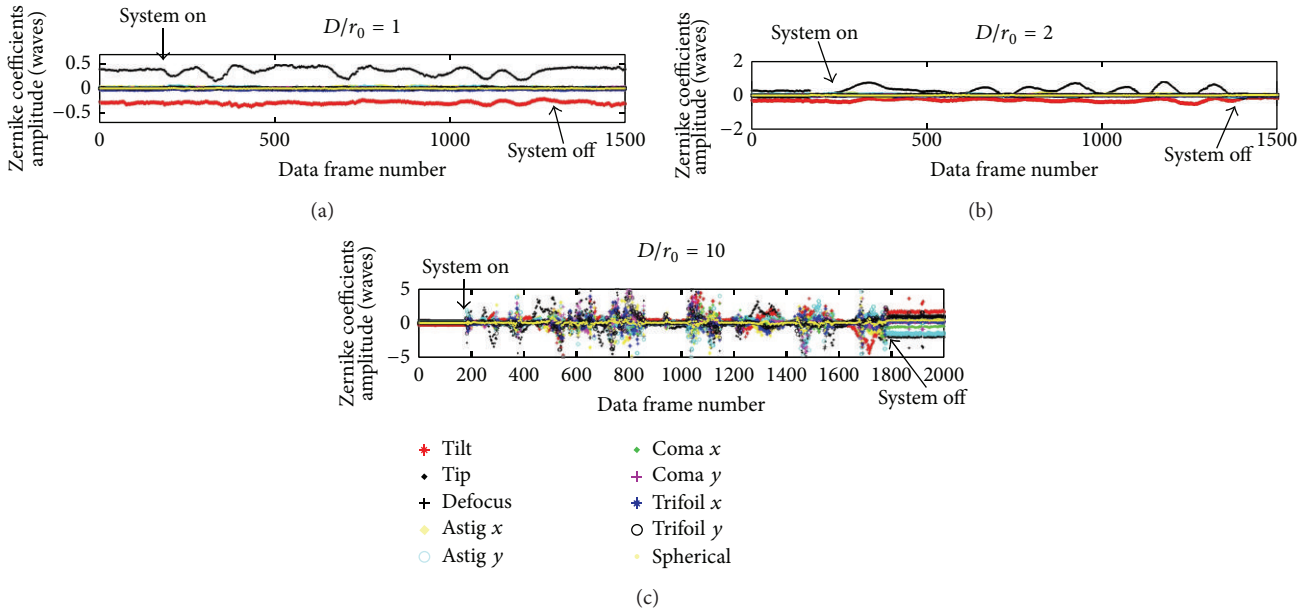

FIGURE 9: Figure shows data recorded by the SHWFS for different D/r_0 values. These ratios represent different atmospheric turbulence conditions ($D/r_0 = 1$, 2, and 10). The plot graphs the variations in amplitudes for the Zernike coefficients as measured per frame (30 fps).

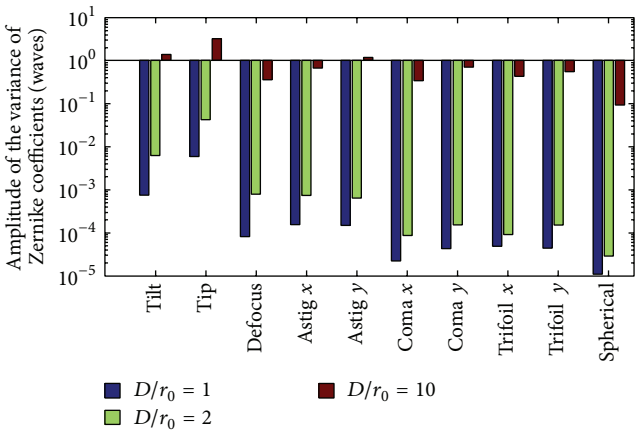

FIGURE 10: This bar plot shows a more quantitative comparison of the behavior of the specific Zernike Orders per each test. The histogram unamibiguously shows the impact of a decreased diameter with respect to r_0. Specifically, for example, when r_0 is ten times greater than the diameter of the receiving telescope, the variance in tip is nearly three orders of magnitude greater than when the diameters of the two are matched ($D/r_0 = 1$).

effects are the limitations that FSLC and other optical systems face in the real world, where the turbulence degrades their performances.

5. Conclusion

This paper shows the progress in the development of a phase only ATS which performs in the SWIR wavelength regime based on a reflective LCSLM. The presented data shows the different degrees of turbulence, from weak to strong, that can be achieved in a controlled environment.

A system like this can greatly contribute to our understanding of how specific degrees of turbulence translate to aberrations which in turn impact propagation of a laser beam through the atmosphere as well as testing the current state of the art. These studies experimentally validate the tool using 1550 nm, which is a principal wavelength used in free space laser-based data links.

Conflict of Interests

The authors declare that there is no conflict of interests regarding the publication of this paper.

References

[1] M. Roggemann and B. Welsh, *Imaging Through Turbulence*, CRC Press, New York, NY, USA, 1996.

[2] L. Andrews and R. Phillips, *Laser Beam Propagation Through Random Media*, SPIE, Bellingham, Wash, USA, 2005.

[3] G. Batchelor, *The Theory of Homogeneous Turbulence*, Cambridge University Press, Cambridge, UK, 1953.

[4] U. Frisch, *Turbulence*, Cambridge University Press, 1995.

[5] C. Wilcox, J. Andrews, S. Restaino, T. Martinez, and S. Teare, "Atmospheric turbulence generator using a liquid crystal spatial light modulator," in *Proceedings of the IEEE Aerospace Conference Digest*, Big Sky, Mont, USA, March 2007.

[6] C. C. Wilcox, *Optical Phase Aberration Generation Using a Liquid Crystal Spatial Light Modulator*, The University of New Mexico, Albuquerque, NM, USA, 2009.

[7] S. R. Restaino, "On the use of liquid crystals for adaptive optics," in *Optical Applications of Liquid Crystal*, L. Vicari, Ed., O&E Series, pp. 118–147, IOP Press, 2005.

[8] J. D. Schmidt, M. E. Goda, and B. D. Duncan, "Aberration production using a high-resolution liquid-crystal spatial light modulator," *Applied Optics*, vol. 46, no. 13, pp. 2423–2433, 2007.

[9] C. Font, D. Bonanno, H. Long et al., "Implementation of a phase only spatial light modulator for an atmospheric turbulence simulator at the short wavelength infrared regime," in *Proceedings of the SPIE Micro- and Nanotechnology Sensors, Systems, and Applications IV*, April 2012.

[10] C. Wilcox, S. Restaino, S. Teare, and T. Martinez, "Adaptive optical system testbed with karhunen-loeve polynomial based method for simulating atmospheric turbulence," U. S. Patent 8,725,471, 2014.